Optik 158 (2018) 237–242

Contents lists available at ScienceDirect

Optik

journal homepage: www.elsevier.de/ijleo

Characterization of trap centers in Gd_2O_3 nanoparticles by low temperature thermoluminescence measurements

S. Delice[a,*], M. Isik[b], N.M. Gasanly[c,d]

[a] Department of Physics, Hitit University, 19040 Çorum, Turkey
[b] Department of Electrical and Electronics Engineering, Atilim University, 06836 Ankara, Turkey
[c] Department of Physics, Middle East Technical University, 06800 Ankara, Turkey
[d] Virtual International Scientific Research Centre, Baku State University, 1148 Baku, Azerbaijan

ARTICLE INFO

Article history:
Received 16 November 2017
Accepted 19 December 2017

Keywords:
Gd_2O_3
Thermoluminescence
Traps

ABSTRACT

Trapping centers in Gd_2O_3 nanoparticles were investigated using thermoluminescence (TL) measurements in the below room temperature region of 10–280 K. Seven peaks having peak maximum temperatures between 30 and 252 K were observed in the TL spectra measured at constant heating rate of 0.3 K/s. Activation energies, order of kinetics and frequency factors were reported using three different analysis techniques: curve fitting, initial rise and peak shape methods. Activation energies of the trapping centers were found between 0.012 eV and 0.79 eV. Most of the TL transitions associated with observed peaks were found as dominated by mixed order of kinetics. Structural characterization of used nanoparticles was achieved using x-ray diffraction and scanning electron microscopy experiments.

1. Introduction

Gd_2O_3, one of the members of lanthanide oxide group, has been an effective material in luminescence applications due to its properties such as thermal stability, low phonon energy ($\sim$600 cm^{-1}), photochemical stability. Moreover, Gd_2O_3 is also a very suitable host material for doping in high ratios thanks to its high density (ρ = 7.6 g/cm^3) and high band gap energy of 5.4 eV. The interest on Gd_2O_3 nano structures has been increasing in recent years since they have potential usage effectiveness in different luminescence applications such LED, lasers, display devices [1–4].

In recent years, studies on doped and undoped Gd_2O_3 nanoparticles focus on their luminescence properties. The properties of energy levels existing due to the presence of defects and/or doping are the most important factor determining the luminescence characteristics of Gd_2O_3 nanophosphors. Transitions between the energy levels lead to different emissions such as red, blue, green, ultraviolet from Gd_2O_3 nanophosphors [5–8]. For that reason it takes importance for technological applications to reveal the properties of these energy levels called as trapping centers in the forbidden band gap. When the studies in literature on the investigations of these energy levels were looked through, it is seen that almost all studies are on the revealing of properties of deep energy levels. Previously, Gd_2O_3 nanophosphors have been investigated in the above room temperature region by thermoluminescence measurements. TL glow curves of Gd_2O_3 nanoparticles synthesized by solution combustion method under four different conditions exhibited one peak around 230 °C [9]. Activation energies of the trap centers were reported between 0.665 and 0.920 eV. Gd_2O_3 phosphors synthesized using conventional solid state

* Corresponding author.
E-mail address: serdardelice@hitit.edu.tr (S. Delice).

https://doi.org/10.1016/j.ijleo.2017.12.102
0030-4026/

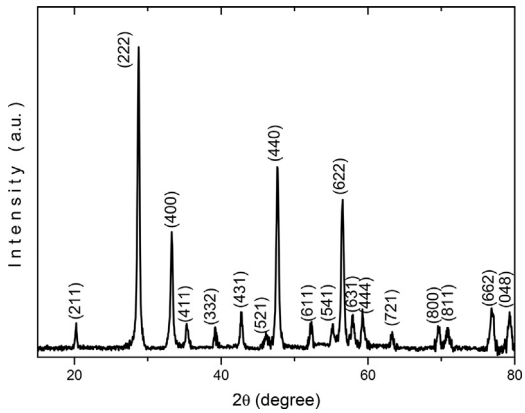

Fig. 1. XRD pattern of Gd_2O_3 nanoparticles.

reaction and combustion synthesis methods were irradiated in TL measurements with UV and gamma sources [10]. The glow curves of nanophosphors synthesized using solid state reaction method presented peaks around 123 and 228 °C under UV and gamma radiations, respectively, while peaks appeared around 103 and 232 °C under UV and gamma radiations, respectively, for samples synthesized using combustion synthesis methods. To the best of our knowledge, there is only one paper on low temperature TL properties of Gd_2O_3 nanophosphors which is doped with europium [11]. TL spectra of Gd_2O_3:Eu nanophosphors indicated peaks around 48, 77, 98, 125, 137, 198 and 280 K. The aim of the present study is to reveal the trapping parameters (activation energy, frequency factor, kinetic order) of Gd_2O_3 nanoparticles using low temperature (10–280 K) thermoluminecence measurements of shallow trap center(s) which is a blank in literature. Structural properties of nanoparticles were also investigated using x-ray diffraction and scanning electron microscopy experiments.

2. Experimental details

Undoped Gd_2O_3 nanoparticles used for TL experiments were supplied from Alfa Aesar. The structural properties of samples were investigated using x-ray diffraction (XRD) and scanning electron microscopy (SEM) experiments. XRD measurements were carried out in the $10^\circ \leq 2\theta \leq 80^\circ$ region using Rigaku Miniflex diffractometer with CuKα radiation ($\lambda = 0.154049$ nm) working at a scanning speed of 0.02 °/sec. Analyses of the experimental data were accomplished using least-squares computer program "DICVOL 04″. Surface morphology of Gd_2O_3 nanoparticles were recorded using JSM-6400 scanning electron microscope.

Low temperature TL measurements were performed using home-made experimental set-up in our luminescence laboratory. A closed cycle helium gas cryostat (Advanced Research Systems, Model CSW-202) was used to get low temperature system. LakeShore Model 331 temperature controller was used to control the sample temperature and to increase the temperature of the sample from 10 to 280 K at a constant heating rate. Sample was illuminated at low temperature using deuterium source (Ocean Optics; D-2000 Deuterium Light Source) producing light in the wavelength range of 215–400 nm. A photomultiplier tube (Hamamatsu R928; spectral response: 185 to 900 nm), a fast amplifier/discriminator (Hamamatsu Photon Counting Unit C3866) and a data acquisition module (National Instruments, NI-USB 6211) were used to measure and count the emitted luminescence. Whole used devices were controlled by a computer using software written in LabView (National Instruments) graphical development environment.

3. Results and discussion

Fig. 1 indicates the x-ray diffraction pattern of Gd_2O_3 nanoparticles in the 2θ range of 10–80°. Presence of sharp diffraction peaks in the pattern is a powerful indication of good crystallinity of the nanoparticles. The lattice parameters of the crystal structure Gd_2O_3 nanoparticles were revealed as cubic structure with lattice parameter of $a = 1.0810$ nm. Moreover, Miller indices of the peaks indicated on the peaks in the figure were obtained from the used software. The obtained lattice parameter is in good agreement with previously reported value of $a = 1.08048$ nm [12] and Miller indices are well correlated with those given in JCPDS card with no of 12–0797 [13]. The diffraction peaks observed in XRD pattern can also be utilized to get information about the particle size. For this purpose, Debye-Scherrer's expression given as [14]

$$D = \frac{0.9\lambda}{\beta \cos\theta} \tag{1}$$

was used. In the equation, D, β and θ symbolize crystalline size, full-width at half maximum and diffraction angle, respectively. The particle size was calculated around 55 nm using Eq. (1).

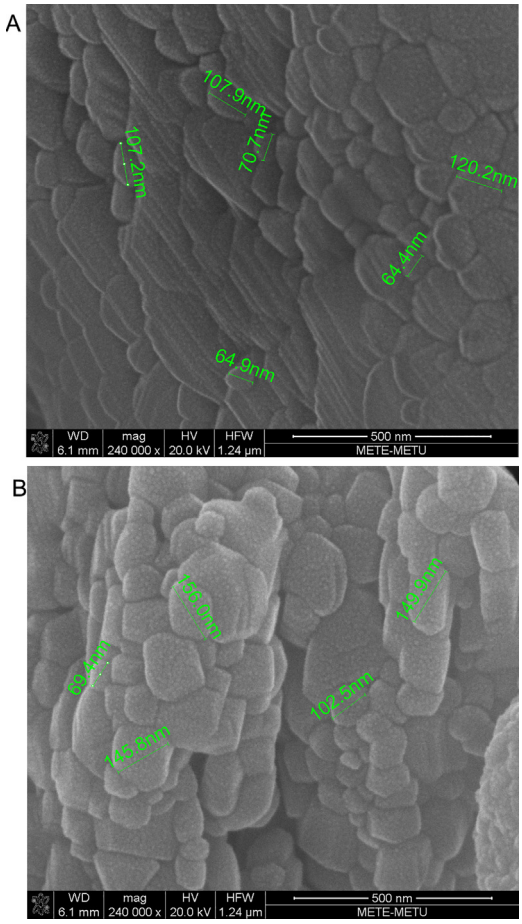

Fig. 2. SEM images of Gd_2O_3 nanoparticles.

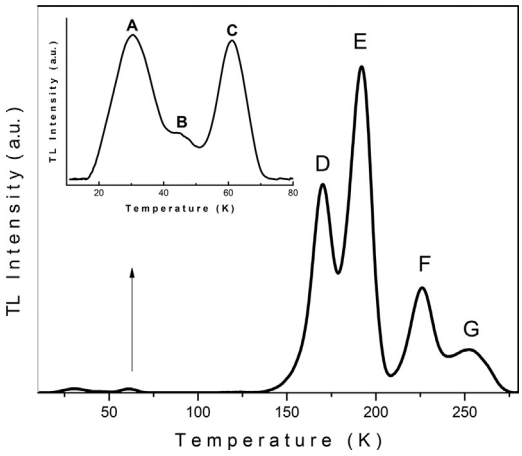

Fig. 3. TL glow curve of Gd_2O_3 nanoparticles for a heating rate of 0.3 K/s.

Scanning electron microscopy (SEM) technique was applied to get information about the surface morphology of Gd_2O_3 nanoparticles. Fig. 2 indicates the SEM images of Gd_2O_3 nanoparticles used as powder form in measurements. As can be seen from the figure, used samples are in the form of nanoparticles having particle size generally in the range of 60–160 nm.

Thermoluminescence experiments carried out on Gd_2O_3 nanoparticles at heating rate of $\beta = 0.3$ K/s resulted in spectra given in Fig. 3. In the 10–80 K temperature range, three overlapped weak peaks around 30, 45 and 61 K and in the 125-275 K range, four overlapped peaks having high intensity around 170, 192, 225 and 253 K were observed. Activation energies (E_t),

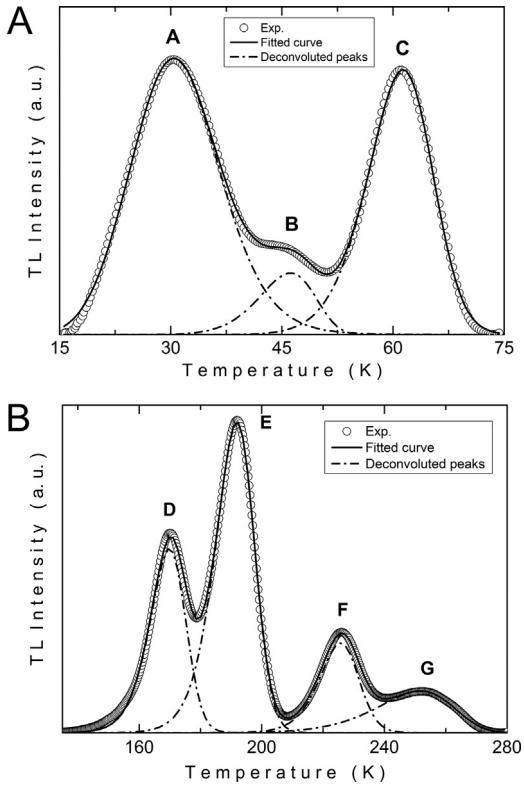

Fig. 4. Experimental TL spectrum (circles) of Gd_2O_3 nanoparticles and decomposition of the curve into separate peaks (dash-dotted curves). (a) and (b) figures represent two different regions of spectrum. Solid curve shows the total fit to the experimental curve.

frequency factors (s) and order of kinetics (b) were determined using different analysis techniques such as curve fit, initial rise and peak shape methods.

Curve fitting method is based on the fitting process of experimental data under the light of theoretical expressions relating TL intensity to temperature. TL curve is the result of radiative recombination of charge carriers emitted from trapping centers. However, there are two ways for an emitted charge from a trap level. It can either be trapped again or make recombination without trapping one more time. The situation in which emitted charges recombine is called as slow retrapping (first order of kinetics) and $b = 1$. If the emitted charge is trapped again before recombination, this is the case of fast retrapping (second order of kinetics) in which $b = 2$. The third case is the mixture of slow and fast retrapping and called as mixed order of kinetics ($1 < b < 2$). The theoretical expressions of TL intensity are given as [15,16]

$$I_{TL} = n_0 s \exp\{-\frac{E_t}{kT} - \int_{T_0}^{T} \frac{s}{\beta} \exp(-E_t/kT)dT\} \text{ (first order kinetics)} \tag{2}$$

$$I_{TL} = n_0 s \exp(-\frac{E_t}{kT})[1 + (b-1)\frac{s}{\beta}\int_{T_0}^{T} \exp(-E_t/kT)dT]^{-\frac{b}{b-1}} \quad \text{(for non-first order kinetics)} \tag{3}$$

where n_o is the initial concentration of trapped charge carriers and T_0 is the starting temperature of heating process. The application of curve fitting technique was given in detail in Ref. [17]. The fitting processes were attempted for each of order of kinetics. Fig. 4 indicates the experimental (circles), fitted (solid line) and deconvoluted (dash dotted line) curves. As can be seen from the figure, experimental spectrum is well-matched with fitted curve. Activation energies of seven different trapping centers were found between 0.012 and 0.79 eV (see Table 1). Dominant mechanism were found as first order for traps B and G, and mixed order for other trapping centers. Order of kinetics are also reported in the table. For the first order of kinetics, curve fitting method also gives opportunity to calculate frequency factor using the activation energy, heating rate and peak maximum temperature [18]. Frequency factors were calculated for peaks B and G as 6.0×10^3 and 6.9×10^6 s^{-1}, respectively.

Initial rise method is another powerful method using the initial rising region of the TL curve. According to Eqs. (2) and (3), the integrals will be negligible for the initial portion of the TL curve. As a result, TL intensity is proportional to $-E_t/kT$ in

Table 1
Peak maximum temperatures (T_m), activation energies (E_t), characteristic parameter (μ_g), order of kinetics (b) and frequency factors (s) for revealed trapping centers before and after thermal cleaning.

	Peak	T_m (K)	E_t (meV)			μ_g	b	s
			Curve fit method	Initial rise method	Peak shape method			
Before cleaning	A	30.4	0.012	0.011	0.014	0.50	1.24	—
	B	46.2	0.045	—	—	—	1.00	6.0×10^3
	C	61.4	0.076	—	0.088	0.48	1.19	—
	D	169.9	0.48	0.46	—	—	1.28	—
	E	191.8	0.55	—	0.56	0.44	1.24	—
	F	225.7	0.79	—	—	—	1.34	—
	G	251.7	0.42	—	—	—	1.00	6.9×10^6
After cleaning	C	62.1	0.069	0.067	0.081	0.49	1.24	—
	F	220.0	0.78	0.76	—	—	1.80	—
	G	251.2	0.44	—	—	—	1.00	2.0×10^7

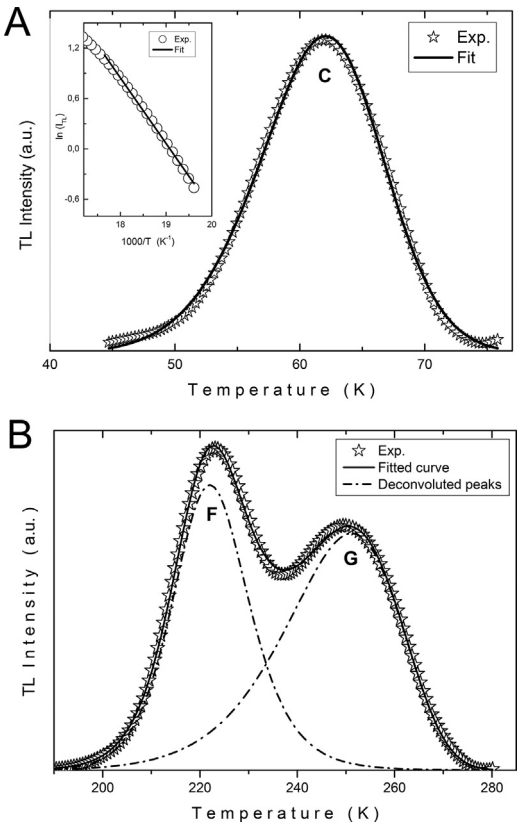

Fig. 5. Experimental (stars) TL curves after thermal cleaning (a) at $T_{cl.} = 34$ K, (b) at $T_{cl.} = 160$ K. Solid lines and dash-dotted curves show total fit and deconvoluted peaks, respectively.

this region for all order of kinetics [15]. However, overlapping peaks restrict the usage of this method since initial rising part of the peaks cannot be read from the TL curve. In the Fig. 4, it can be detected that initial rising regions of peak A and D are not affected from other peaks. The slope of logarithm of TL intensity vs. $1/T$ graph was used to calculate associated activation energies of trapping centers which were found as $E_{tA} = 0.011$ eV and $E_{tD} = 0.46$ eV. These results show a good consistency with those obtained from curve fitting method.

Peak shape method also called as Chen method analyze temperature values of T_m, T_l and T_h which symbolize the peak maximum, low and high half intensity temperatures, respectively [15]. One restriction to apply this method is that these temperature values must be obtained from TL curve for individual peaks. Overlapping peaks can damage this condition, if T_m, T_l and T_h values cannot be read from TL curve. In addition to determination of activation energy, this method also gives information about the order of kinetics responsible for TL transitions. Chen and Kirsh [15] predict the value of characteristic parameter $\mu_g = (T_h - T_m)/(T_h - T_l)$ as 0.42 for first-order kinetics, 0.52 for second-order kinetics and between these values for mixed order of kinetics for an individual peak. When the association of deconvoluted peaks with experimental curve were taken into consideration, it is seen that half intensity temperatures for peaks A, C and E can be read from the spectrum. Peak

shape method analyses resulted in activation energies of E_{tA} = 0.014 eV, E_{tC} = 0.088 eV and E_{tE} = 0.56 eV and characteristic parameters of μ_{gA} = 0.50, μ_{gC} = 0.48 and μ_{gE} = 0.44 which correspond the mixed order of kinetics values. All obtained values were reported in Table 1.

Thermal cleaning is an experimental technique performed to separate overlapped peaks. The applied analyses methods give more reliable outputs when the number of overlapped peaks was decreased. The procedure of this experimental approach is carried out as following: The sample is illuminated at low temperature (T = 10 K) and after waiting a few minutes in dark to bring the charge carriers in equilibrium, sample is heated at a constant heating rate. Instead of heating the sample to high limit temperature, heating process is cut at a temperature value called as cleaning temperature ($T_{cl.}$) which depletes the trapping centers below and around T_{cl}. Then the sample is cooled to initial temperature and sample is heated without additional illumination. The obtained TL spectrum after this process presents the peaks associated with remaining unaffected traps from T_{cl}. Fig. 5a and b show the observed TL glow curves when thermal cleaning procedure was applied for $T_{cl.}$ = 34 K and $T_{cl.}$ = 160 K, respectively. As can be seen from Fig. 5a, observed TL peak belongs to peak C while peaks in Fig. 5b is related to trapping centers of F and G. Experimentally cleaned TL curves were analyzed using above given methods. Table 1 presents the trapping center parameters obtained as a results of applied techniques. The comparison of activation energies before and after thermal cleaning shows that all revealed values are in good agreement with each other.

4. Conclusion

Gd_2O_3 nanoparticles were investigated using structural characterization techniques and thermoluminescence measurements. X-ray diffraction analyses revealed the crystal structure as cubic with lattice parameter of a = 1.0810 nm. SEM images indicated that used samples are in the form of nanoparticles with size around 60–160 nm. TL experiments were performed in the temperature range of 10–280 K illuminating the sample with a deuterium source. TL spectra indicated the presence of seven trapping centers having activation energies between 0.012 and 0.79 eV. The order of kinetics were found between 1.00 and 1.34. Frequency factors of traps located at 0.045 and 0.42 eV associated with first order of kinetics were found as 6.0×10^3 and 6.9×10^6 s^{-1}, respectively. Thermal cleaning procedure was also applied to separate some overlapped peaks.

References

[1] K.S. Singh, K. Kumar, S.B. Rai, Optical properties and switching behavior in Gd_2O_3:Er^{3+} nanophosphor, J. Appl. Phys. 106 (2009) 093520.
[2] N. Dhananjaya, H. Nagabhushana, B.M. Nagabhushana, B. Rudraswamy, C. Shivakumara, R.P.S. Chakradhar, Effect of Li^{3+} -ion on enhancement of photoluminescence in Gd_2O_3:Eu^{3+} nanophosphors prepared by combustion technique, J. Alloy. Compd. 509 (2011) 2368–2374.
[3] S. Duenas, H. Castan, H. Garcia, A. Gomez, L. Bailon, K. Kukli, T. Hatanpaa, J. Lu, M. Ritala, M. Leskela, Electrical properties of atomic-layer-deposited thin gadolinium oxide high-k gate dielectrics, J. Electrochem. Soc. 154 (2007) G207–G214.
[4] C.H. Kao, H. Chen, Y.T. Pan, J.S. Chiu, S.P. Lin, C.S. Laia, The investigation of the high-k Gd2O3 (gadolinium oxide) interdielectrics deposited on the polycrystalline silicon, J. Electrochem. Soc. 157 (2010) H915–H918.
[5] M. Jayasimhadri, B.V. Ratnam, K. Jang, H.S. Lee, Combustion synthesis and luminescent properties of nano and Submicrometer-Size Gd_2O_3:Dy^{3+} phosphors for white LEDs, Appl. Ceram. Technol. 8 (2011) 709–717.
[6] R.K. Tamrakar, D.P. Bisen, N. Brahme, Effect of Yb^{3+} concentration on photoluminescence properties of cubic Gd_2O_3 phosphor, Infrared Phys. Techn. 68 (2015) 92–97.
[7] Y. Li, G. Hong, Y. Zhang, Y. Yu, Red and gren upconversion luminescence of Gd_2O_3:Er^{3+}, Yb^{3+} nanoparticles, J. Alloy Compd. 456 (2008) 247–250.
[8] H. Guo, N. Dong, M. Yin, W. Zhang, L. Lou, S. Xia, Visible upconversion in rare earth ion-doped Gd_2O_3 nanocrystals, J. Phys. Chem. B 108 (2004) 19205–19209.
[9] N. Dhananjaya, H. Nagabhushana, B.M. Nagabhushana, B. Rudraswamy, S.C. Sharma, D.V. Sunitha, C. Shivakumara, R.P.S. Chakradhar, Effect of different fuels on structural, thermo and photoluminescent properties of Gd_2O_3 nanoparticles, Spectrochim. Acta A-M 96 (2002) 532–540.
[10] R.K. Tamrakar, D.P. Bisen, K. Upadhyay, I.P. Sahu, Comparative study of thermoluminescence behaviour of Gd_2O_3 phosphor synthesized by solid state reaction and combustion method with different exposure, Radiat. Meas. 84 (2016) 41–54.
[11] Y. Wang, O. Milosevic, L. Gomez, M.E. Rabanal, J.M. Torralba, B. Yang, P.D. Townsend, Thermoluminescence responses from europium doped gadolinium oxide, J. Phys.-Condens. Mat. 18 (2006) 9257–9272.
[12] E.L. Correa, B. Bosch-Santos, F.H.M. Cavalcante, B.S. Correa, R.S. Freitas, A.W. Carbonari, M.P.A. Potiens, Properties of Gd_2O_3 nanoparticles studied by hyperfine interactions and magnetization measurements, AIP Adv. 6 (2016) 056112.
[13] JCPDS (Joint Committee on Powder Diff ;raction Standart) Card no: 12-0797.
[14] B.D. Cullity, S.R. Stock, Elements of X-ray Diffraction, Prentice Hall, New Jersey, 2001.
[15] R. Chen, Y. Kirsh, Analysis of Thermally Stimulated Processes, Pergamon Press, 1981.
[16] A.J.J. Bos, Theory of Thermoluminescence, Radiat. Meas. 41 (2006) S45–S56.
[17] M. Isik, K. Goksen, N.M. Gasanly, H. Ozkan, Trap distribution in TlInS2 layered crystals from thermally stimulated current measurements, J. Korean Phys. Soc. 52 (2008) 367–373.
[18] R. Chen, S.W.S. McKeever, Theory of Thermoluminescence and related phenomena, World Scientific, 1997.